

PHYSICS

Toroidal optical transitions in hydrogen-like atoms

Ilya Kuprov¹, David Wilkowski^{2,3,4*}, Nikolay Zheludev^{2,5,6}

It is commonly believed that electromagnetic spectra of atoms and molecules can be fully described by interactions involving electric and magnetic multipoles. However, it has recently become clear that interactions between light and matter also involve toroidal multipoles—toroidal absorption lines have been observed in electromagnetic metamaterials. Here, we show that a previously unexplored type of spectroscopy of the hitherto largely neglected toroidal dipolar interaction becomes feasible if, apart from the classical $\mathbf{r} \times \mathbf{r} \times \mathbf{p}$ toroidal dipole density term responsible for the toroidal transitions in metamaterials, the spin-dependent $\mathbf{r} \times \boldsymbol{\sigma}$ term (which only occurs in relativistic quantum mechanics) is taken into account. Toroidal dipole operators are odd under parity and time-reversal symmetries; toroidal dipole transitions can therefore be distinguished from electric multipole and magnetic dipole transitions.

INTRODUCTION

The description of electromagnetic properties of matter traditionally involves multipole expansions (1, 2) that are widely used in the study of biological, chemical, atomic, and subatomic phenomena, where electromagnetic processes are described by electric and magnetic multipoles arising from moving charges and current loops. Toroidal multipoles (3), generated by currents flowing on toroidal surfaces, constitute the rarely acknowledged third independent family of vector potential sources; they provide distinct and essential contributions to electromagnetic properties of matter.

Static toroidal dipoles (Fig. 1, top right) were introduced in 1957 by Zeldovich (4); they are found in magnetic materials (5), atomic nuclei (6, 7), single-molecule magnets (8), fullerenes (9), and in solid-state physics (10). Dynamic toroidal dipoles with oscillating currents interact with oscillating electromagnetic fields and thus contribute to optical properties of matter. They were first observed in artificial metamaterials (11); in recent years, they made appearances in various forms of artificially structured matter across the electromagnetic spectrum: metamaterials (12), nanoparticles (13), discussions of noise-resistant quantum devices (14), dynamic anapoles (15, 16), dark matter (17–19), communication using Aharonov-Bohm effect (20, 21), electromagnetic reciprocity (22), and as contributors to nonradiating charge-current configurations (15, 20). Recently observed electromagnetic pulses of toroidal topology, the propagating counterparts of localized toroidal dipole excitations in matter, exhibit unique electromagnetic wave properties (23, 24).

The work on dynamic toroidal multipoles has so far mainly involved Maxwell electromagnetic metamaterials, and the associated spin effects have therefore been overlooked (3). However, those are unavoidable in quantum mechanical systems, such as atoms and molecules—Dirac's equation only conserves the sum of orbital angular momentum and spin (25). In this communication, we consider the possibility of using spin effects to open new toroidal

excitation channels. We demonstrate that using the nonrelativistic toroidal dipole operator $\mathbf{r} \times \mathbf{r} \times \mathbf{p}$ is exceedingly difficult due to field frequency-curvature mismatch and selection rules that make the transition hard to distinguish from more regular electromagnetic transitions. However, the appearance of the spin part $\mathbf{r} \times \boldsymbol{\sigma}$ in the relativistic case eliminates the frequency-curvature problem and yields selection rules that involve spin; this makes the corresponding transitions easier to isolate from the background. We identify pairs of energy levels and experimental conditions for which toroidal transitions in hydrogen-like atoms are likely to be detectable.

RESULTS

Nonrelativistic case: Vector potential curvature problem

The length scale of electronic optical transitions of interest in atomic physics, chemistry, and molecular biology is typically two to four orders shorter than the wavelength of light. This creates a problem for a hypothetical spectroscopy based on the classical $\mathbf{r} \times \mathbf{r} \times \mathbf{p}$ toroidal dipole—we demonstrate here that significant electric field curvature

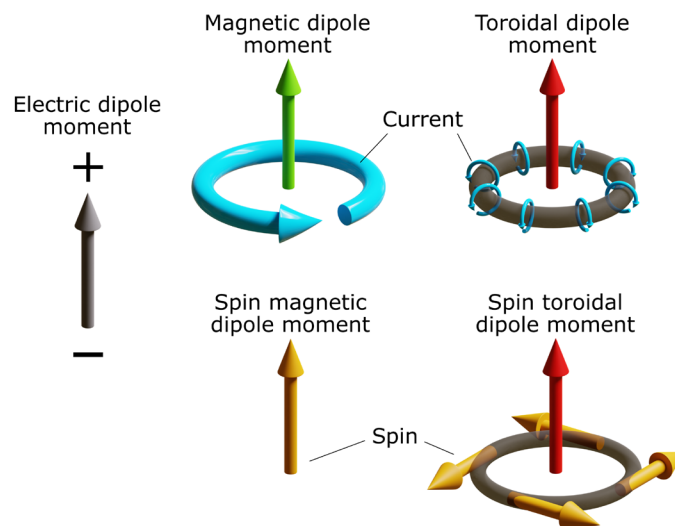


Fig. 1. Schematic illustrations of static electric, magnetic, and toroidal dipoles in classical electrodynamics. In relativistic quantum physics, apart from magnetic and toroidal moments induced by charge currents, spin must be considered because it can also contribute to the toroidal dipole moment.

¹School of Chemistry, University of Southampton, Southampton, UK. ²Centre for Disruptive Photonic Technologies, SPMS, The Photonics Institute, Nanyang Technological University, Singapore 637371, Singapore. ³Centre for Quantum Technologies, National University of Singapore, Singapore 117543, Singapore. ⁴MajuLab, International Joint Research Unit IRL 3654, CNRS, Université Côte d'Azur, Sorbonne Université, National University of Singapore, Nanyang Technological University, Singapore, Singapore. ⁵Optoelectronics Research Centre, University of Southampton, Southampton, UK. ⁶Hagler Institute for Advanced Studies, Texas A&M University, College Station, TX 77843, USA.

*Corresponding author. Email: david.wilkowski@ntu.edu.sg

is required on the molecular length scale and that the optimal frequency-wavelength combination for $\mathbf{r} \times \mathbf{r} \times \mathbf{p}$ spectroscopy is three orders of magnitude away from the constraint imposed by the speed of light.

For an electron in a scalar potential $\varphi(\mathbf{r})$ and a vector potential $\mathbf{A}(\mathbf{r})$, the Hamiltonian, in the Coulomb gauge, can be split into the background term \hat{H}_0 and the coupling term \hat{H}_1 (1)

$$\hat{H}_0 = \frac{\mathbf{p}^2}{2m} - e\varphi + \frac{e^2}{2m} \mathbf{A} \cdot \mathbf{A}, \quad \hat{H}_1 = \frac{e}{m} \mathbf{A} \cdot \mathbf{p} \quad (1)$$

where m is the electron mass, and e is the elementary charge. The two electromagnetic operators appearing in \hat{H}_0 are not interesting to us here—they are purely coordinate operators that cannot contain anything proportional to $\mathbf{r} \times \mathbf{r} \times \mathbf{p}$.

In the coupling term \hat{H}_1 , consider an electromagnetic plane wave with a vector potential amplitude \mathbf{A}_0 and angular frequency ω , traveling in the direction of a unit vector \mathbf{n}

$$\mathbf{A}(\mathbf{r}, t) = \mathbf{A}_0 \exp [i(\omega/c) \mathbf{n} \cdot \mathbf{r} - i\omega t] \quad (2)$$

The toroidal operator originates in the Taylor expansion of the spatial part

$$\exp [i(\omega/c) \mathbf{n} \cdot \mathbf{r}] = 1 + i(\omega/c) \mathbf{n} \cdot \mathbf{r} - (\omega/c)^2 (\mathbf{n} \cdot \mathbf{r})^2 / 2 + \dots \quad (3)$$

for which straightforward vector calculus transformations yield

$$(\mathbf{n} \cdot \mathbf{r})^2 \mathbf{p} = \mathbf{r}(\mathbf{r} \cdot \mathbf{p}) - ((\mathbf{n} \times \mathbf{r}) \cdot (\mathbf{n} \times \mathbf{r})) \mathbf{p} - \mathbf{r} \times \mathbf{r} \times \mathbf{p} \quad (4)$$

Although electronic transitions under $\mathbf{r} \times \mathbf{r} \times \mathbf{p}$ operator are possible—a direct calculation confirms that there are plenty of nonzero transition moments within the orbital structure of any reasonable molecule—the conclusions regarding the sensitivity and selectivity of such transitions are pessimistic. First, there are electric and/or magnetic operators in every irreducible representation of the rotation group, meaning that any allowed $\mathbf{r} \times \mathbf{r} \times \mathbf{p}$ transition will overlap with an electric or a magnetic transition of exactly the same frequency. Second, $\mathbf{r} \times \mathbf{r} \times \mathbf{p}$ term in the plane wave expansion in Eq. 3 is a factor of $(\omega r/c)^2 = (2\pi r/\lambda)^2$ —here, r is the characteristic size of the molecular orbitals in question— weaker than the zero-order term responsible for the electric dipolar interaction, meaning that the transition rate in the Fermi golden rule is a factor of $(2\pi r/\lambda)^4$ smaller. For common atom sizes ($\sim 10^{-10}$ m) and a wavelength in ultraviolet, we expect a typical $\mathbf{r} \times \mathbf{r} \times \mathbf{p}$ transition rate to be a factor of 10^{11} weaker than a typical electric dipolar transition rate.

These are likely the reasons why toroidal transitions have never been observed in chemical spectroscopies. So far, dynamic toroidal excitations have only been seen in metamaterials, where resonant structures with the feature size comparable to the wavelength can be engineered in such a way that $2\pi r/\lambda \approx 1$, and the lower order electric and magnetic multipoles suppressed by design (3, 11).

Relativistic case: Spin part of the toroidal operator

We now consider an important difference between Maxwell electromagnetic metamaterials and molecules: The orbital angular momentum $\mathbf{r} \times \mathbf{p}$ that occurs in the $\mathbf{r} \times \mathbf{r} \times \mathbf{p}$ is only a constant of motion in the rotation subgroup of the Galilean group. The corresponding

invariant in Lorentz and Poincare groups also includes relativistic boosts, leading to the conservation of the sum of orbital angular momentum and spin. The corresponding $\hbar(\mathbf{r} \times \boldsymbol{\sigma})$ correction to the toroidal operator, where $\boldsymbol{\sigma}$ is a vector of Pauli matrices, clearly should be evaluated.

In the standard derivation of the electromagnetic and spin Hamiltonian by approximate elimination of negative energies from Dirac's equation, the first occurrence of the $\mathbf{r} \times \boldsymbol{\sigma}$ product is in the angular magnetoelectric (AME) part (26) of the gauge invariant form of spin-orbit (SO) coupling

$$\hat{H}_{\text{SO+AME}} = -\frac{e\hbar}{4m^2c^2} \boldsymbol{\sigma} \cdot [(\nabla\varphi) \times (\mathbf{p} + e\mathbf{A})] \quad (5)$$

The conventional SO term is not interesting to us here—it comes from the scalar potential—but the triple product with the vector potential is easily rearranged into a form that exposes the presence of the spin part of the toroidal operator

$$\hat{H}_{\text{AME}} = \frac{e^2\hbar}{4m^2c^2} \mathbf{A} \cdot [(\nabla\varphi) \times \boldsymbol{\sigma}] \quad (6)$$

This is directly visible in the special case of a hydrogen-like atom with a nuclear charge Z

$$\nabla\varphi(\mathbf{r}) = -\frac{Ze}{4\pi\epsilon_0} \frac{\mathbf{r}}{r^3} \quad (7)$$

where the spin part $\mathbf{r} \times \boldsymbol{\sigma}$ of the toroidal dipole moment is coupled to the vector potential

$$\hat{H}_{\text{AME}} = -\frac{\alpha\mu_B^2}{ec} \frac{Z}{r^3} \mathbf{A} \cdot [\mathbf{r} \times \boldsymbol{\sigma}] \quad (8)$$

where α is the fine structure constant, and μ_B is the Bohr magneton. This was previously considered a spin interaction (26); the form presented here views it instead as pertaining to the relativistic component of the toroidal dipole moment.

Selection rules

Although the interaction described by Eq. 8 is exceedingly weak, its transitions are nonetheless expected to be observable because their selection rules are different from the selection rules associated with electric and magnetic dipoles (Table 1). The corresponding operators are

$$\mathbf{d} \propto \mathbf{r}, \quad \boldsymbol{\mu}_S \propto \mathbf{S}, \quad \mathbf{t}_S \propto \mathbf{r} \times \mathbf{S} \quad (9)$$

where \mathbf{d} stands for electric dipole, $\boldsymbol{\mu}_S$ stands for the spin part of magnetic dipole, \mathbf{t}_S stands for the spin part of the toroidal dipole, and the electron spin operator is $\mathbf{S} = \hbar\boldsymbol{\sigma}/2$. In each specific SO multiplet of a hydrogen-like atom, the total magnetic moment is proportional, by Wigner-Eckart theorem, to the total momentum $\mathbf{J} = \mathbf{L} + \mathbf{S}$.

The spin part is critical because $\Delta m_s = \pm 1$ in combination with $\Delta L = \pm 1$ transitions are only excited through the toroidal coupling and not through electric or magnetic dipole moments. Although its operator has the same symmetry, the hypothetical spin-independent magnetic quadrupole moment of the atom would only interact with magnetic field gradient of the electromagnetic wave and would therefore have, for the same reasons, even lower observability than $\mathbf{r} \times \mathbf{r} \times \mathbf{p}$ transitions discussed above. Electron spin does not contribute to the magnetic quadrupole moment of a spherical atom

Table 1. Selection rules for electric, magnetic, and toroidal dipolar transitions in a hydrogen-like atom. L , m_l , and m_s are, respectively, the orbital quantum number, the orbital projection quantum number, and the spin projection quantum number. For magnetic and toroidal dipole moments, the photon polarization either changes the orbital angular momentum or flips the spin, and therefore, $\Delta m_j \leq 1$ (37).

Moment	Parity symmetry	Time-reversal symmetry	Orbital selection rule	Spin selection rule	J selection rule
Electric dipole	Odd	Even	$\Delta L = \pm 1, \Delta m_l = 0, \pm 1$	$\Delta m_s = 0$	$\Delta J = 0, \pm 1, \Delta m_j = 0, \pm 1$
Magnetic dipole	Even	Odd	$\Delta L = 0, \Delta m_l = 0, \pm 1$	$\Delta m_s = 0, \pm 1$	$\Delta J = 0, \pm 1, \Delta m_j = 0, \pm 1$
Toroidal dipole	Odd	Odd	$\Delta L = \pm 1, \Delta m_l = 0, \pm 1$	$\Delta m_s = 0, \pm 1$	$\Delta J = 0, \pm 1, \Delta m_j = 0, \pm 1$

because electron spin is fundamentally a point magnetic dipole. Similar arguments apply to other multipoles and their cross terms.

DISCUSSION

We now show that toroidal dipole transitions can be observed in hydrogen-like atoms when the spin projection m_s is a good quantum number. In practice, this means Paschen-Back regime: strong static magnetic field and weak fine structure interaction. We will skip the consideration of nuclear spin because the transitions in question conserve nuclear spin orientation.

Consider a hydrogen-like atom exposed to a plane electromagnetic wave with circular polarization propagating along the z axis, here chosen as the quantization axis. $\mathbf{B} = B\hat{\epsilon}_\pm$ is the optical magnetic field, and $\hat{\epsilon}_\pm$ is a unit vector corresponding to the two possible signs of circular polarization. The interaction Hamiltonian in Eq. 8 becomes

$$\hat{H}_{\text{AME}}(\hat{\epsilon}_\pm) = \pm \frac{\alpha}{\sqrt{2}} \frac{\mu_B^2}{ec} \frac{Z}{r^3} \frac{B}{k} (\rho e^{\pm i\varphi} \boldsymbol{\sigma}_Z - z \boldsymbol{\sigma}_\pm) \quad (10)$$

where φ is the azimuthal angle, ρ is the radial position operator, k is the wave number, and $\boldsymbol{\sigma}_\pm = \boldsymbol{\sigma}_X \pm \boldsymbol{\sigma}_Y$. The last term is of particular interest because $z\boldsymbol{\sigma}_\pm$ simultaneously flips the spin and drives spatial orbital transitions with $\Delta L = \pm 1$. In principle, this makes highly transition-selective multiple-quantum filtered spectroscopies possible because spin can also be manipulated separately, with very high precision, using microwave pulses.

Consider now $n^2S_{1/2} \rightarrow n'^2P_{3/2,1/2}$ transition for which the energies are shown in Fig. 2 as functions of the external static magnetic field $\mathbf{B}_{\text{DC}} = B_{\text{DC}}\hat{z}$. The transitions $|m=0, m_s = \pm 1/2\rangle_g \rightarrow |m=0, m_s = \mp 1/2\rangle_e$ (black dashed arrows) are only toroidal dipole allowed.

In a zero magnetic field, SO coupling partially lifts the excited state degeneracy and makes j a good quantum number (27). This situation is not suitable for observation of toroidal transitions because toroidal transitions then coincide in energy with the much stronger electric dipole ones. However, in strong magnetic fields, orbital and spin quantum numbers again become independent, and toroidal transitions become distinguishable.

State mixing (green arrows in Fig. 2) decreases as $\epsilon = \Delta E_{\text{FS}}/2\mu_B B_{\text{DC}}$, where ΔE_{FS} is the fine structure energy splitting; toroidal transition rate exceeds electric dipolar transition rate when

$$\frac{|\langle 0, \mp 1/2 | H_{\text{AME}} | 0, \pm 1/2 \rangle|^2}{\epsilon^2 |\langle \mp 1, \pm 1/2 | H_E | 0, \pm 1/2 \rangle|^2} \approx \frac{1}{2} \left(\frac{\alpha a_0 k}{\epsilon} \right)^2 > 1 \quad (11)$$

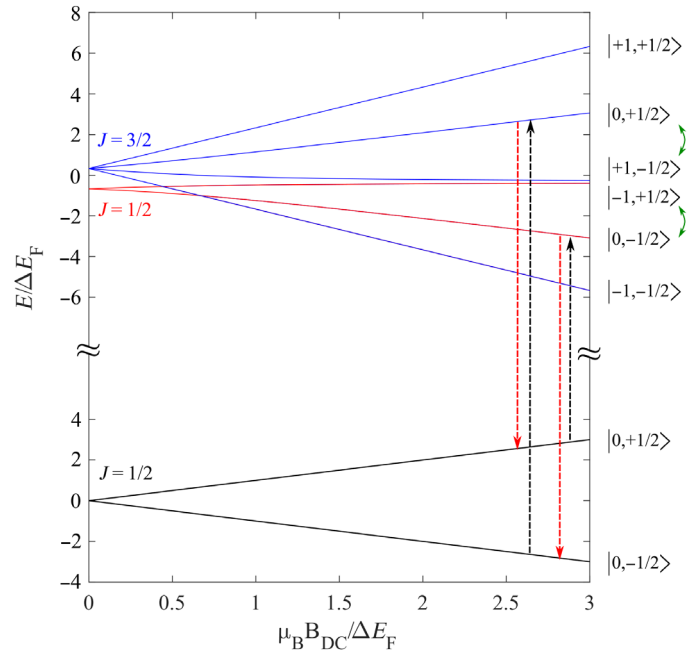


Fig. 2. Energy spectrum of the transition $n^2S_{1/2} \rightarrow n'^2P_{3/2,1/2}$ as a function of the static magnetic field B_{DC} . Black, red, and blue curves correspond to the ground state, to $J = 1/2$ excited state manifold, and $J = 3/2$ excited state manifold in the $B_{\text{DC}} \rightarrow 0$ limit, respectively. Black dashed arrows indicate the toroidal transition; red dashed arrows indicate the electric dipole allowed primary de-excitation route. The quantum numbers in brackets refer to orbital angular momentum (first) and spin (second) projection, in the $B_{\text{DC}} \rightarrow +\infty$ limit. Green double arrows indicate state mixing due to fine structure coupling.

where a_0 is the Bohr radius, and $H_E = -\mathbf{d} \cdot \mathbf{E}$ is the electric dipole Hamiltonian. Thus, the most easily observable toroidal transitions are likely to be those with small ΔE_{FS} . For hydrogen-like atoms $\Delta E_{\text{FS}} \approx \alpha^4 mc^2 Z^2 / 4n'^3$, which is favorable for light atoms and states with high principal quantum numbers. For actual hydrogen at $B_{\text{DC}} = 5$ T, the inequality in Eq. 11 is fulfilled for the $n' \approx 51$ Rydberg state and above, which may be addressed from $n = 2$ (Balmer series) with a continuous wave laser at a wavelength around 364 nm. This wavelength is available by doubling frequency of a tuneable Ti:Sapphire laser, for example. The fundamental laser may be frequency-locked on an optical frequency comb to get a precise and tuneable optical frequency.

Although its frequency is now different, the toroidal transition moment is around $\frac{1}{2}(\alpha a_0 k)^2 \approx 2 \cdot 10^{-11}$ times smaller than the electric dipole transition moment. We therefore propose the following practical measures to make its observation possible:

1) Frequency-modulation spectroscopy should be used to detect the weak resonance against the background signal coming from the off-resonance nearby electric dipole transitions (28).

2) Because de-excitation occurs mainly over inelastic electric dipole allowed transitions, appropriate frequency filtering of the fluorescence signal should be performed to remove the spurious signal at the excitation frequency.

3) Hydrogen atoms could be replaced by lithium atoms, which also have favorable fine structure splitting (29). There, we can consider excitations from the fundamental ground state but deeper into the ultraviolet part of the spectrum.

4) Toroidal dipole coupling operator is odd under time-reversal symmetry. It therefore changes sign under a change of the static magnetic field sign (equivalent to a flip in the light polarization state in Eq. 10), whereas the electric dipole operator remains unaffected. Hence, the experiment may be conducted in a differential mode, where the toroidal contribution is extracted from the difference in absorption between the experiments conducted with $B_{DC} > 0$ and $B_{DC} < 0$ or in a way similar to the recent measurement of parity nonconservation in caesium (7).

In high magnetic fields, diamagnetic response operators (which scale as B^2) are also expected to become pertinent because they mix the principal and the orbital quantum numbers (30). This breaks the selection rules in Table 1 and could therefore impose extra conditions on the optimal magnetic field and the choice of atoms for observation of toroidal excitations.

Last, it is important to emphasize the difference between the well-characterized static nuclear toroidal moments that contribute, for example, to the parity-violating transition between the 6S and 7S states of caesium (7) and the dynamic spin-dependent toroidal interactions between electromagnetic waves and the electronic structure or atoms that are explored in this work.

REFERENCES AND NOTES

1. P. W. Atkins, R. S. Friedman, *Molecular Quantum Mechanics* (Oxford Univ. Press, 2011).
2. F. Jensen, *Introduction to Computational Chemistry* (John Wiley & Sons, 2017).
3. N. Papisimakis, V. A. Fedotov, V. Savinov, T. A. Raybould, N. I. Zheludev, Electromagnetic toroidal excitations in matter and free space. *Nat. Mater.* **15**, 263–271 (2016).
4. Y. B. Zel'dovich, Electromagnetic interaction with parity violation. *J. Exp. Theor. Phys.* **33**, 1184–1186 (1957).
5. I. S. Zheludev, T. M. Perekalina, E. M. Smirnovskaya, S. S. Fonton, Y. N. Yarmukhamedov, Magnetic properties of the nickel-iodine boracite. *JETP Lett.* **20**, 289–292 (1974).
6. W. Haxton, C.-P. Liu, M. J. Ramsey-Musolf, Nuclear anapole moments. *Phys. Rev. C* **65**, 045502 (2002).
7. C. Wood, S. C. Bennett, D. Cho, B. P. Masterson, J. L. Roberts, C. E. Tanner, C. E. Wieman, Measurement of parity nonconservation and an anapole moment in caesium. *Science* **275**, 1759–1763 (1997).
8. J. Goura, E. Colacio, J. M. Herrera, E. A. Sutorina, I. Kuprov, Y. Lan, W. Wernsdorfer, V. Chandrasekhar, Heterometallic Zn_3Ln_3 ensembles containing (μ_6 -CO₃) ligand and triangular disposition of Ln^{3+} ions: Analysis of single-molecule toric (SMT) and single-molecule magnet (SMM) Behavior. *Chemistry* **23**, 16621–16636 (2017).
9. A. Ceulemans, L. Chibotaru, P. Fowler, Molecular anapole moments. *Phys. Rev. Lett.* **80**, 1861 (1998).
10. V. Dubovik, V. Tugushev, Toroid moments in electrodynamics and solid-state physics. *Phys. Rep.* **187**, 145–202 (1990).
11. T. Kaelberer, V. A. Fedotov, N. Papisimakis, D. P. Tsai, N. I. Zheludev, Toroidal dipolar response in a metamaterial. *Science* **330**, 1510–1512 (2010).
12. T. Raybould, V. A. Fedotov, N. Papisimakis, I. Kuprov, I. J. Youngs, W. T. Chen, D. P. Tsai, N. I. Zheludev, Toroidal circular dichroism. *Phys. Rev. B* **94**, 035119 (2016).
13. A. E. Miroshnichenko, A. B. Evlyukhin, Y. F. Yu, R. M. Bakker, A. Chipouline, A. I. Kuznetsov, B. Luk'yanchuk, B. N. Chichkov, Y. S. Kivshar, Nonradiating anapole modes in dielectric nanoparticles. *Nat. Commun.* **6**, 8069 (2015).
14. A. M. Zagoskin, A. Chipouline, E. Il'ichev, J. R. Johansson, F. Nori, Toroidal qubits: Naturally-decoupled quiet artificial atoms. *Sci. Rep.* **5**, 16934 (2015).
15. V. A. Fedotov, A. V. Rogacheva, V. Savinov, D. P. Tsai, N. I. Zheludev, Resonant transparency and non-trivial non-radiating excitations in toroidal metamaterials. *Sci. Rep.* **3**, 2967 (2013).
16. V. Savinov, N. Papisimakis, D. P. Tsai, N. I. Zheludev, Optical anapoles. *Commun. Phys.* **2**, 69 (2019).
17. A. Alves, A. C. O. Santos, K. Sinha, Collider detection of dark matter electromagnetic anapole moments. *Phys. Rev. D* **97**, (2018).
18. C. M. Ho, R. J. Scherrer, Anapole dark matter. *Phys. Lett. B* **722**, 341–346 (2013).
19. D. C. Latimer, Anapole dark matter annihilation into photons. *Phys. Rev. D* **95**, (2017).
20. N. A. Nemkov, A. A. Basharin, V. A. Fedotov, Nonradiating sources, dynamic anapole, and Aharonov-Bohm effect. *Physical Review B* **95**, (2017).
21. E. A. Marengo, R. W. Ziolkowski, Nonradiating sources, the Aharonov-Bohm effect, and the question of measurability of electromagnetic potentials. *Radio Sci.* **37**, 19-1–19-10 (2002).
22. G. N. Afanasiev, Simplest sources of electromagnetic fields as a tool for testing the reciprocity-like theorems. *J. Phys. D Appl. Phys.* **34**, 539–559 (2001).
23. A. Zdagkas, Y. Shen, C. McDonnell, J. Deng, G. Li, T. Ellenbogen, N. Papisimakis, N. I. Zheludev, Observation of toroidal pulses of light. *Nat. Photon.* **16**, 523–528 (2022).
24. Y. Shen, Y. Hou, N. Papisimakis, N. I. Zheludev, Supertoroidal light pulses as electromagnetic skyrmions propagating in free space. *Nat. Commun.* **12**, 5891 (2021).
25. P. A. M. Dirac, *The Principles of Quantum Mechanics* (Oxford Univ. Press, 1981).
26. R. Mondal, M. Berritta, C. Paillard, S. Singh, B. Dkhil, P. M. Oppeneer, L. Bellaiche, Relativistic interaction Hamiltonian coupling the angular momentum of light and the electron spin. *Phys. Rev. B* **92**, 100402 (2015).
27. L. D. Landau, E. M. Lifshitz, *Quantum Mechanics: Non-Relativistic Theory* (Elsevier, 2013), vol. 3.
28. G. C. Bjorklund, Frequency-modulation spectroscopy: A new method for measuring weak absorptions and dispersions. *Opt. Lett.* **5**, 15–17 (1980).
29. W. Wiese, J. Fuhr, Accurate atomic transition probabilities for hydrogen, helium, and lithium. *J. Phys. Chem. Ref. Data* **38**, 565–720 (2009).
30. L. Schiff, H. Snyder, Theory of the quadratic Zeeman effect. *Phys. Rev.* **55**, 59–63 (1939).
31. S. Hayami, M. Yatsushiro, Y. Yanagi, H. Kusunose, Classification of atomic-scale multipoles under crystallographic point groups and application to linear response tensors. *Phys. Rev. B* **98**, 165110 (2018).

Acknowledgments

Funding: This work was supported by the U.K. Engineering and Physical Sciences Research Council (EP/M009122/1), the Singapore Ministry of Education (MOE2016-T3-1-006 and MOE-T2EP50120-0005), European Research Council (FLEET-786851), and the Defense Advanced Research Projects Agency (DARPA) under the Nascent Light Matter Interactions program. N.Z. acknowledges support from Hagler Institute for Advances Study, Texas A&M University. **Author Contributions:** I.K. provided the quantum mechanical description of toroidal spectroscopy; D.W. evaluated applicability conditions of toroidal spectroscopy; N.I.Z. conceived the idea; all co-authors discussed the results and contributed to writing the manuscript. **Competing interests:** The authors declare they have no competing interests. **Data and materials availability:** All data needed to evaluate the conclusions in the paper are present in the paper.

Submitted 23 April 2022

Accepted 21 September 2022

Published 9 November 2022

10.1126/sciadv.abq6751